Switchable solvent-based liquid micro-extraction in combination with magnetic solid micro-extraction for determination of Diphenhydramine Hydrochloride in pharmaceutical preparations

Hiba Qasem Kadhim,
sci.chem.mas.23.9@qu.edu.iq
Zeina M. Kadam
zeina.m.kadam@qu.edu.iq
*Department of Chemistry, College of Science, University of Al-Qadisiyah, Diwaniyah, Iraq.
Tel : +9647831813693

Abstract

This study presents a novel and environmentally friendly microextraction method for the determination of diphenhydramine hydrochloride (DPH). The method integrates switchable hydrophilicity solvent-based liquid–liquid microextraction (SHS-LLME) with magnetic solid-phase extraction (MSPE). Initially, Fe_3O_4 magnetic nanoparticles were synthesized through co-precipitation and functionalized with oleic acid to enhance colloidal stability and prevent agglomeration. The structural and magnetic properties of the nanoparticles were characterized using X-ray diffraction (XRD), transmission electron microscopy (TEM), field emission scanning electron microscopy (FESEM), vibrating sample magnetometry (VSM), and Fourier-transform infrared spectroscopy (FTIR). These analyses confirmed successful modification of the nanoparticles without altering their core crystalline structure. In the SHS-LLME step, N,N-dimethyl cyclohexylamine (DMCA) served as the switchable solvent, with its polarity adjusted by using hydrochloric acid (HCl) and sodium hydroxide (NaOH). Following this, the MSPE procedure employed Fe_3O_4@oleic acid as the sorbent to isolate DPH from the organic phase. Various critical variables affecting extraction performance—including the type and volume of solvent, volumes of acid and base, temperature, amount of sorbent, desorption solvent, volume, and time—were optimized using a one-variable-at-a-time (OVAT) approach. Under optimal conditions, the method demonstrated excellent linearity over a concentration range of 2.5–25 mg/L ($R^2 = 0.9996$). The limits of detection and quantification were determined to be 1.30 mg/L and 3.95 mg/L, respectively. This technique achieves a high preconcentration factor with reduced solvent consumption, aligning with the principles of green analytical chemistry. Consequently, the combined SHS-LLME/MSPE method enables efficient, selective, and reproducible measurement of DPH in pharmaceutical preparations, making it suitable for routine drug quality control applications.

Keywords: Diphenhydramine Hydrochloride، Switchable Hydrophilicity Solvent (SHS)، Fe_3O_4 Nanoparticles، Oleic Acid Coating، Magnetic Solid-Phase Extraction (MSPE)

الاستخلاص الدقيق القابل للتحويل باستخدام المذيبات السائلة مع الاستخلاص الدقيق المغناطيسي للمواد الصلبة لتحديد هيدروكلوريد ديفينهيدرامين في المستحضرات الصيدلانية

هبة قاسم كاظم
sci.chem.mas.23.9@qu.edu.iq
زينة م. كاظم
zeina.m.kadam@qu.edu.iq
*قسم الكيمياء، كلية العلوم، جامعة القادسية، الديوانية، العراق.
هاتف: 9647831813693+

الملخص

تقدم هذه الدراسة طريقة استخلاص دقيق جديدة وصديقة للبيئة لتحديد هيدروكلوريد ديفينهيدرامين (DPH). تدمج هذه الطريقة الاستخلاص الدقيق القابل للتحويل باستخدام المذيبات السائلة (SHS-LLME) مع الاستخلاص المغناطيسي للطور الصلب (MSPE). في البداية، تم تصنيع جسيمات نانوية مغناطيسية Fe_3O_4 من خلال الترسيب المشترك، ووظيفتها مع حمض الأوليك لتعزيز الاستقرار الغرواني ومنع التكتل. وُصفت الخصائص البنيوية والمغناطيسية للجسيمات النانوية باستخدام حيود الأشعة السينية(XRD) ، والمجهر الإلكتروني النافذ(TEM) ، والمجهر الإلكتروني الماسح بالانبعاث الميداني(FESEM) ، وقياس مغناطيسية العينة المهتزة(VSM) ، ومطيافية الأشعة تحت الحمراء بتحويل فورييه (FTIR). أكدت هذه التحليلات نجاح تعديل الجسيمات النانوية دون تغيير بنيتها البلورية الأساسية. في خطوة SHS-LLME ، كان N,N-ثنائي ميثيل سيكلوهكسيل أمين (DMCA) بمثابة المذيب القابل للتبديل، مع تعديل قطبيته باستخدام حمض الهيدروكلوريك (HCl) وهيدروكسيد الصوديوم (NaOH). بعد ذلك، استخدمت عملية MSPE Fe_3O_4@حمض الأوليك كمادة ماصة لعزل DPH من الطور العضوي. تم تحسين العديد من المتغيرات الحرجة المؤثرة على أداء الاستخلاص، بما في ذلك نوع وحجم المذيب، وحجم الحمض والقاعدة، ودرجة الحرارة، وكمية المادة الماصة، ومذيب الامتزاز، والحجم، والوقت، باستخدام نهج "متغير واحد في كل مرة" (OVAT). في ظل الظروف المثلى، أظهرت الطريقة خطية ممتازة على نطاق تركيز يتراوح بين 2.5 و25 ملغم/لتر ($R^2 = 0.9996$). حُددت حدود الكشف والقياس الكمي لتكون 1.30 ملغم/لتر و3.95 ملغم/لتر على التوالي. تحقق هذه التقنية عامل تركيز مسبق مرتفع مع انخفاض استهلاك المذيبات، بما يتماشى مع مبادئ الكيمياء التحليلية الخضراء. وبالتالي، تُمكّن طريقة SHS-LLME/MSPE المدمجة من قياس DPH بكفاءة وانتقائية وقابلية للتكرار في المستحضرات الصيدلانية، مما يجعلها مناسبة لتطبيقات مراقبة جودة الأدوية الروتينية.

الكلمات المفتاحية: هيدروكلوريد ديفينهيدرامين، مذيب قابل للتبديل محب للماء(SHS) ، جسيمات نانوية Fe_3O_4، طلاء حمض الأوليك، استخلاص الطور الصلب المغناطيسي(MSPE)

1 Introduction:

Diphenhydramine hydrochloride is 2 -(diphenyl methoxy)-N, N-dimethyl ethylamine hydrochloride. A common antiallergic, antiemetic, and antitussive, a histamine H1-receptor antagonist. It comes in a variety of pharmaceutical formats that are usually used orally, such as tablets, capsules, and syrups. It can also be injected intramuscularly or intravenously in situations of severe allergies.(1) Numerous analytical techniques, such as spectrophotometry(2), have been reported for the determination of DPH in pharmaceutical formulations(3).(4) (5)Flow Injection Analysis(6) The electrophoresis of capillaries(7). (8)Thin layer chromatography.(9)Chromatography of gas(10)High-performance liquid chromatography(11).(12)Traditional sample preparation techniques, such as liquid-liquid extraction (LLE) and solid-phase extraction (SPE), are often time-consuming, labor-intensive, and require large amounts of organic solvents, raising environmental and health concerns(13).(14)Miniaturized and environmentally friendly techniques have garnered increasing attention in analytical chemistry. One such innovative method is switchable solvent-based liquid-phase microextraction (SS-LLME). This technique uses solvents that can reversibly transition between being miscible and immiscible with water, depending on external stimuli like pH or carbon dioxide levels.(15)This adaptable behavior reduces solvent consumption, improves selectivity, and enables efficient analyte partitioning. However, when an external magnetic field is added, functionalized magnetic nanoparticles are used in magnetic solid-phase extraction (MSPE), which enables the quick and precise separation of analytes from complicated mixtures(16).(17)The integration of SS-LPME with MSPE (Magnetic Solid-Phase Extraction) creates a hybrid extraction strategy that combines the adaptability of switchable solvents with the high surface area and magnetically driven recovery of solid sorbents. This method improves enrichment factors, reduces sample handling, and aligns with the principles of green analytical chemistry.Currently, there has been limited research on the use of this dual-extraction technique for determining diphenhydramine hydrochloride (DPH). Therefore, this study aims to develop and optimize a combined SS-LPME/MSPE method for the sensitive and selective extraction of DPH.

2 Experimental

2.1 Instruments:

Various analytical and laboratory instruments were employed throughout this study to ensure accurate characterization and effective analysis. The instruments used, along with their models, manufacturers, and locations, are described below: A Field Emission Scanning Electron Microscope (FE-SEM), model MIRA3 from TESCAN (Czech Republic), was utilized for surface morphology analysis and was operated in Iran. A Transmission Electron Microscope (TEM), model A12AB from Leo (Germany), was also used in Iran to investigate the internal structure and particle size of the synthesized materials. The X-ray Diffractometer (XRD), model XRD-6000, manufactured by Shimadzu (Japan), was employed for crystallographic analysis and operated in Iran as well. To investigate functional groups and confirm chemical structures, a Fourier Transform Infrared Spectrophotometer (FT-IR), model FT-IR84005 (Shimadzu, Japan), was used at the University of Al-Qadisiya, College of Science. Additionally, two types of UV-Visible Spectrophotometers were utilized: a double-beam spectrophotometer (model UV-1650, Shimadzu, Japan) and a single-beam spectrophotometer (model 1200RS, FARLAB, Korea), both located at the same institution. Weighing of samples was carried out using a digital analytical balance, model EP214C (OHAUS, Switzerland), while drying steps were performed using a vacuum oven, model DO-18 (HYSC, Korea), both available at the University of Al-Qadisiyah. Sample mixing and agitation were performed using an orbital shaker (model LSI-I, Labtech, Korea) and a hotplate with magnetic stirrer (model LMS-1003, Labtech, Korea), and sample dispersion and dissolution were enhanced using an ultrasonic bath, model LUC-410 (Shimadzu, Japan). All of these instruments were located at the University of Al-Qadisiya, College of Science.

2.2 Chemicals and reagents:

All solutions were prepared using deionized water. A stock solution of diphenhydramine hydrochloride (50 mg L^{-1}) was prepared by dissolving 0.0025 g of the standard in hot deionized water. The solution was then filtered and diluted to a final volume of 50 mL in a calibrated volumetric flask. The organic solvents utilized in this study—methanol (99.9%), ethanol (99.9%), acetonitrile (99.5%), acetone (99.5%), and toluene (99.9%)—were obtained from Merck (Germany). Ferric chloride hexahydrate ($FeCl_3 \cdot 6H_2O$), ferrous chloride tetrahydrate ($FeCl_2 \cdot 4H_2O$), oleic acid (OA), and aqueous ammonia solution (25%) were purchased from Loba Chemie Pvt. Ltd. (India). The switchable polarity solvents, namely N,N-dimethylcyclohexylamine (DMCA), triethylamine (TEA), and 2-(dibutylamino)ethanol (DBAE), were supplied by Macklin (China).

2.3 Synthesis of Fe3O4 magnetic nanoparticles:

Magnetite (Fe_3O_4) nanoparticles were synthesized via a conventional co-precipitation method. Specifically, 5.6 g of ferric chloride hexahydrate ($FeCl_3 \cdot 6H_2O$) and 2.3 g of ferrous chloride tetrahydrate ($FeCl_2 \cdot 4H_2O$) were dissolved in 50 mL of deionized water under constant magnetic stirring. The solution was then heated to 83 °C under a nitrogen atmosphere. A total of 20 mL of 25% aqueous ammonia solution was added dropwise, leading to the formation of a black precipitate, indicating the successful synthesis of Fe_3O_4 nanoparticles. The resulting nanoparticles were collected by magnetic separation, washed repeatedly with deionized water to remove unreacted ions, and dried at 65 °C(18) .

2.4 Oleic Acid Surface Coating:

"A total of 1.0 g of Fe_3O_4 nanoparticles was dispersed in 20 mL of deionized water via ultrasonication for 2 minutes. Subsequently, 2 mL of oleic acid was added, and the resulting mixture was continuously stirred for 6 hours to achieve surface modification. The functionalized nanoparticles were then magnetically separated, washed thoroughly with ethanol to remove excess reagents, and dried overnight at 85 °C(19).

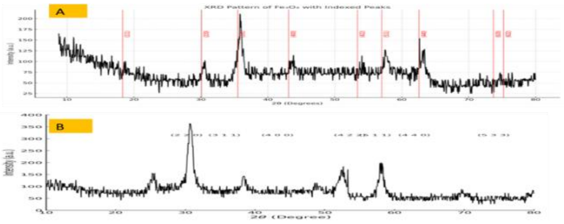

Figure 1: The X-ray diffraction pattern on of the Fe3O4(A)

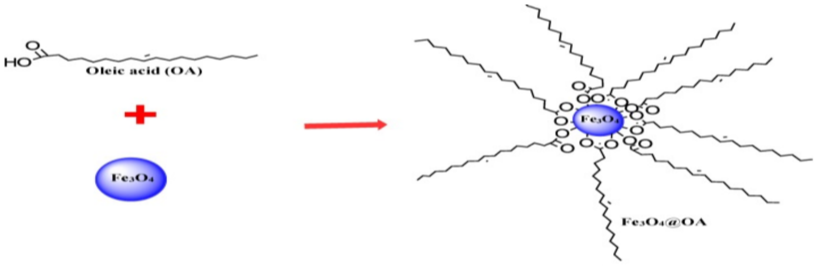

Figure 2 Linking oleic acid to iron oxide nanoparticles(43)

2.5 SHS-Based Liquid-Liquid Microextraction Procedure:

A 3 mL aliquot of the solution containing diphenhydramine hydrochloride was transferred into a 10 mL centrifuge tube. Subsequently, 200 µL of DMCA and 500 µL of 6 mol/L HCl were added, and the mixture was vortexed for 10 seconds. The tube was then placed in a water bath at 50°C for 2 minutes. Phase separation was induced by the addition of 800 µL of 10 mol/L NaOH, resulting in a turbid solution. Finally, the DMCA-rich phase was carefully collected from the aqueous phase surface using a syringe.(20)

2.6 Magnetic solid microextraction procedure:

A 0.01 g amount of Fe_3O_4@oleic acid (Fe_3O_4@OA) sorbent was added to a clean tube containing the obtained SHS phase. The mixture was vortexed for 20 minutes to allow folic acid (FA) to adsorb onto the magnetic material. Following adsorption, the magnetic nanoparticles (MNPs) were rapidly separated from the solution using a strong magnet. Desorption was performed by adding 2 mL of methanol and shaking for 15 minutes. The resulting eluent was then used for UV-Vis spectrophotometric analysis(21).

3 Results and discussion:

3.1 Characterization of Fe3O4@oleic acid nanoparticles

3.1.1 X-Ray Diffraction Analysis (XRD):

Both uncoated Fe_3O_4 nanoparticles (Figure 2A) and OA-coated Fe_3O_4 nanoparticles (Figure 2B) exhibit distinct diffraction peaks at 2θ values of approximately 30.1°, 35.5°, 43.1°, 53.5°, 57.0°, and 62.6°. These peaks correspond to the (220), (311), (400), (422), (511), and (440) planes of the spinel structure of magnetite (Fe_3O_4)(22). This observation demonstrates that the fundamental crystalline structure of Fe_3O_4 remains unchanged even after the OA coating(23).(24) However, these peaks appear broader and less intense in the OA-coated samples. This broadening may result from the surface modification process, indicating a reduction in crystallite size or an increase in lattice strain(25).(26)Oleic acid molecules adhere to the surface of Fe_3O_4 nanoparticles through their carboxylate groups, forming a chemisorbed layer. The absence of additional peaks in the XRD patterns suggests that this organic layer does not create new crystalline phases. Instead, it introduces a slight amount of disorder at the nanoparticle's surface, which results in peak broadening and a decrease in intensity(27). By preventing agglomeration through steric hindrance, the OA coating significantly improves the dispersion stability of nanoparticles. This enhanced dispersion is crucial for applications requiring consistent nanoparticle distribution. The XRD analysis indicates that coating Fe_3O_4 nanoparticles with oleic acid preserves the core spinel structure while causing minor alterations to the surface. The observed changes, such as peak broadening and variations in intensity, are attributed to the formation of an amorphous organic layer on the nanoparticle surface. This layer enhances dispersion without compromising the crystalline integrity of the Fe_3O_4 nanoparticles.

3.1.2 Transmission Electron Microscopy (TEM):

A transmission electron microscopy (TEM) image of iron oxide nanoparticles with a semi-spherical form and obvious aggregation is displayed in Figure 3A. Strong interparticle interactions, such as van der Waals forces and magnetic dipole-dipole attractions, are usually the cause of this clustering. Due to their high surface energy, uncoated magnetic nanoparticles are particularly susceptible to these forces, which encourage agglomeration as a means of lowering the system's overall energy consumption(28). On the other hand, Figure 3B displays the identical nanoparticles following their oleic acid coating. Particle aggregation is greatly decreased by this surface change, leading to a more distributed arrangement. The enhanced dispersion is presumably owing to the steric barrier generated by the oleic acid layer. Since the carboxylic end of its long hydrophobic tail establishes a bond with the iron oxide surface, it creates a physical barrier that prevents direct contact between the nanoparticles(29).(30) It is frequently used to increase colloidal stability and solubility in organic solvents, which is particularly useful in biomedical applications like imaging and medication delivery. Differences in electron density between the organic shell and the iron oxide core could be the cause of the contrast difference between the two TEM images. Because the oleic acid coating has a lower electron density, certain areas of the image have less contrast. Nonetheless, the

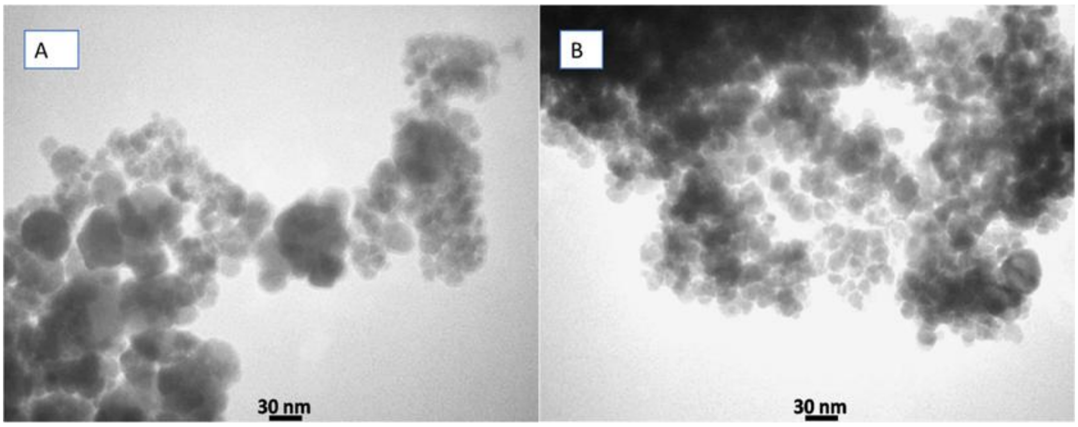

Figure 3 TEM image of Fe3O4(A)Fe3O4@OA

core nanoparticles' general shape doesn't essentially alter. Because of its demonstrated capacity to reduce nanoparticle aggregation through steric stabilization, oleic acid was chosen as a coating agent. Its long hydrophobic tail's carboxylic end forms a strong bond with the iron oxide surface, creating a protective organic shell that improves colloidal stability in organic fluids and blocks direct particle-to-particle interaction. This makes it ideal for enhancing the dispersion of nanoparticles and avoiding agglomeration(29).

3.1.3 field emission scanning electron microscopy (FESEM):

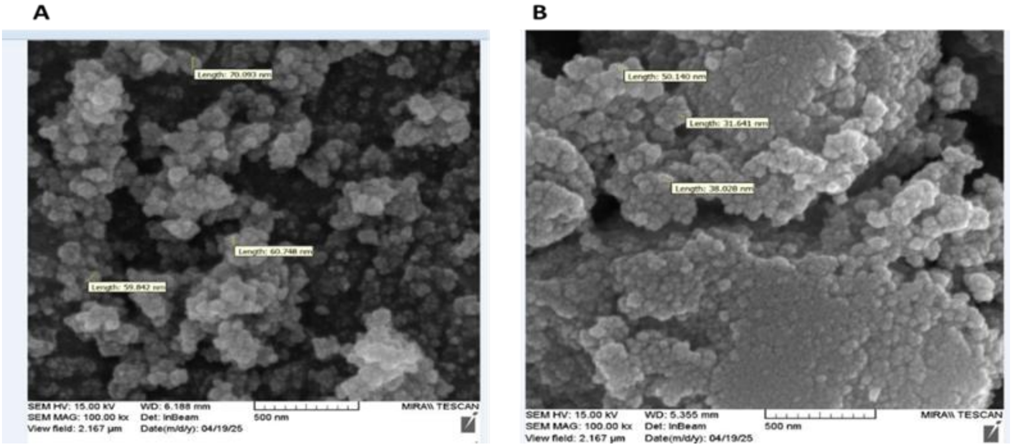

Figure 4 FESEM of Fe3O4 (A) Fe3O4@OA(B)

Figure 4A shows a Field Emission Scanning Electron Microscope (FESEM) image of iron oxide nanoparticles before they have been modified with oleic acid. The particles appear to be aggregated and range in size from 59 to 70 nanometers. The strong van der Waals forces and high surface energy of the nanoparticles contribute to this aggregation when no stabilizing surface coating is present. The scientific literature has extensively demonstrated that nanoscale particles tend to cluster in the absence of protective coverings(31)(32)The FESEM image in Figure 4B shows iron oxide nanoparticles coated with oleic acid, which facilitates the formation of Fe_3O_4. These coated particles exhibit greater dispersion and smaller diameters, ranging from approximately 31 to 50 nanometers, compared to uncoated Fe_3O_4. The oleic acid layer prevents the particles from direct contact with one another, reducing aggregation and enhancing colloidal stability, particularly in organic environments(31). The Fe_3O_4 particles in the oleic acid (OA) photographs display a more uniform size and less aggregation compared to the uncoated particles. The uncoated particles show significant clumping and a broader size distribution. The steric hindrance caused by the lengthy hydrophobic chains of the oleic acid molecules extending outward reduces van der Waals and magnetic interactions. Additionally, a connection is formed between the carboxyl groups of oleic acid and the surface of the Fe_3O_4 particles.(33)The steric hindrance provided by the lengthy hydrocarbon chains of oleic acid is responsible for the enhanced particle dispersion and decreased size shown in the oleic acid-coated nanoparticles. By lowering magnetic interactions and van der Waals forces, this barrier improves the colloidal stability of the particles. The literature has extensively shown such behavior for magnetic nanoparticles coated with oleic acid(34).

3.1.4 Vibrating Sample Magnetometer (VSM):

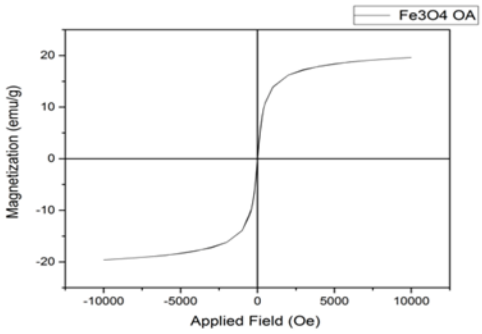

Figure 5 Magnetization curve of Fe3O4(A)Fe3O4@OA(B)

Figure 5illustrates the typical super-paramagnetic behavior seen in the magnetic hysteresis loop of Fe_3O_4 nanoparticles that are coated with oleic acid. This behavior is characterized by very low coercivity (Hc < 1 Oe) and nearly zero remanent magnetization (Mr = 0).(29)Due to surface spin canting and the presence of a non-magnetic oleic acid shell, the saturation magnetization (Ms) of Fe_3O_4 nanoparticles ranges from 54 to 80 emu/g, which is somewhat lower than that of bulk Fe_3O_4. This magnetic behavior is attributed to their small particle size, typically less than 20 nm, which leads to rapid fluctuations in magnetic moments and allows thermal energy to overcome the anisotropic energy barrier. The mechanism of Néel relaxation governs this process. The oleic acid coating acts as a steric stabilizer by reducing interparticle magnetic interactions, preventing agglomeration, and enhancing colloidal stability. These characteristics make Fe_3O_4-OA nanoparticles highly suitable for various biomedical applications, such as magnetic drug targeting, MRI contrast enhancement, and hyperthermia treatment(35).

3.1.5 FTIR Analysis:

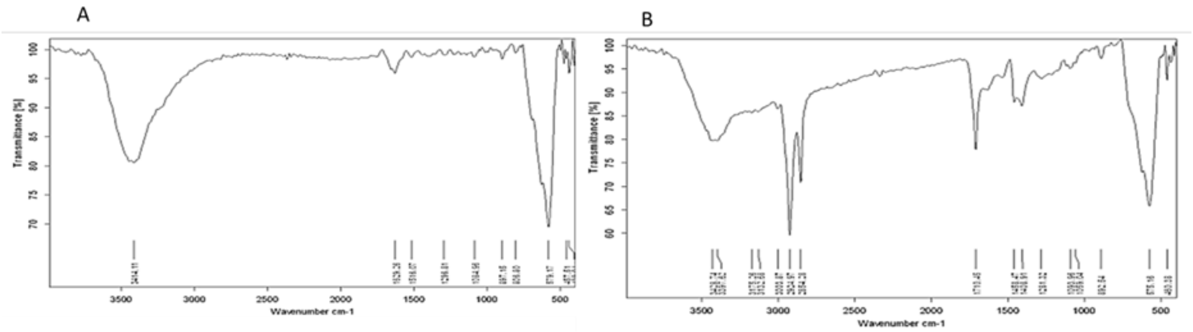

Figure 6: FT-IR spectra of Fe3O4(A) Fe3O4@OA(B)

Figure 6A: Uncoated FeO_4 Nanoparticles

The presence of surface hydroxyl groups and the iron oxide structure is confirmed by distinctive peaks in the FTIR spectrum of uncoated iron oxide nanoparticles:

- The large absorption peak at 3411 cm^{-1} corresponds to the stretching vibrations of -OH groups, which are often associated with surface-adsorbed water or hydroxyl functional groups on the nanoparticles' surface.
- The bending vibrations of H–O–H produce bands in the range of 1629–1566 cm^{-1}, further indicating the presence of adsorbed moisture on the surface.
- The characteristic peaks at 574 cm^{-1} and 432 cm^{-1} confirm the presence of the spinel structure typical of FeO_4, as they correspond to the stretching of the Fe–O bond(36).

Nanoparticles of FeO_4 Coated with Oleic Acid Figure 6B

When the nanoparticles' surfaces are modified with oleic acid, the FTIR spectrum exhibits notable alterations, suggesting that the coating procedure was successful(37). The asymmetric and symmetric stretching vibrations of the CH_2 groups present in the lengthy hydrocarbon chain of oleic acid are linked to the peaks at 2920 and 2850 cm^{-1}.(38)The stretching of the carbonyl group (C=O) from the free–COOH group in unbound oleic acid is represented by the band 1710 cm^{-1}(39). The asymmetric and symmetric stretching vibrations of carboxylate groups ($–COO^-$) appear as peaks at 1533 cm^{-1} and 1441 cm^{-1}. This indicates that coordination with Fe^{2+} ions has led to the chemisorption of oleic acid onto the surface of the nanoparticle. Additionally, the Fe–O band is still detectable at 571 cm^{-1}, suggesting that the magnetic core remains physically intact.

3.2 Optimization Conditions for SHS-LLME Technique:

The switchable hydrophilicity solvent-based liquid-liquid micro-extraction

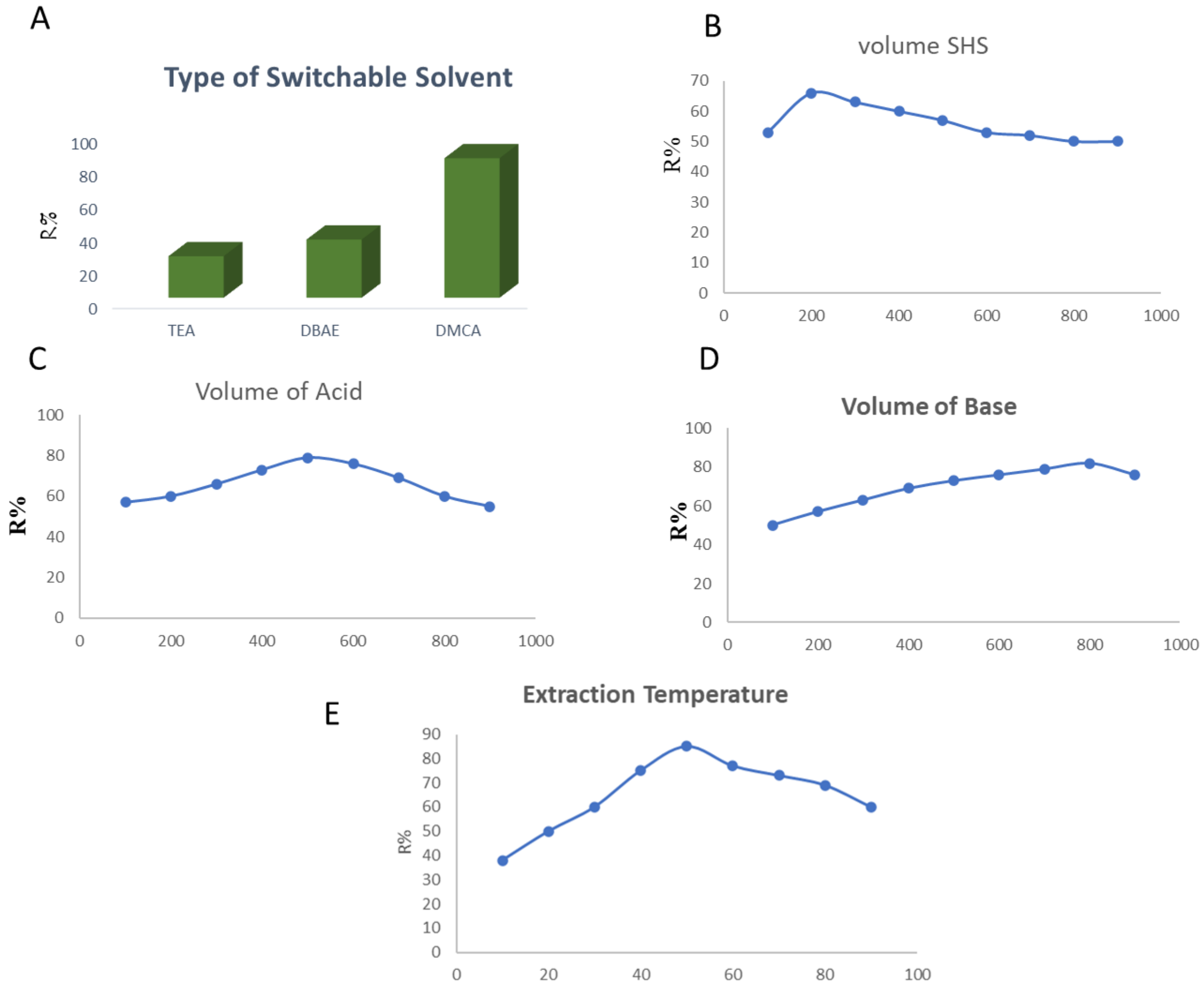

Figure 7 Type of Switchable Solvent(A) Volume of SHS(B) Volume of Acid(C) Volume of Base(D) Extraction Temperature**(E)**

(SHS-LLME) methodology utilizes solvents that can transition between hydrophilic and hydrophobic states in response to environmental stimuli, such as pH. This innovative approach to sample preparation enhances extraction efficiency. We employed a one-variable-at-a-time (OVAT) method to investigate the effects of various critical factors and improve the extraction process for DPH. Our findings indicate that the following conditions are optimal:

3.2.1 Type of Switchable Solvent:

Three tertiary amines were evaluated:

- N, N-Dimethyl cyclohexylamine (DMCA)
- Triethylamine (TEA)
- Dibutylaminoethanol (DBAE)

Due to its favorable log Kow value (which is less than 2.5) that allows for reversible polarity switching, DMCA has been identified as the most efficient solvent. It was selected because of its advantageous physicochemical properties, including low toxicity, moderate solubility in both organic and aqueous phases, and its commercial availability. This indicates that SHS can be effectively developed in line with previous research findings(40), as shown in Figure 7A.

3.2.2 Volume of SHS:

Test volumes of DMCA varied from 100 to 800 µL. Previous research on SHS-based techniques indicated that the best recovery occurred with 200 µL; beyond that volume, dilution effects began to reduce extraction effectiveness(41), as shown in Figure 6 B.

3.2.3 Volume of Acid (HCl):

Hydrochloric acid (6 M) acts as a polarity modulator, converting the solvent into a hydrophilic state. It was found that a volume of 500 µL ensures complete protonation of the solvent, thereby maximizing analyte solubilization (Figure 6C).

3.2.4 Volume of Base (NaOH):

The solvent was converted back to its hydrophobic state, and phase separation was induced using a 10 M sodium hydroxide solution. An amount of 800 µL yielded the best results, as it facilitated an effective phase transition and allowed the analyte to partition into the organic layer (see Figure 6D).

3.2.5 Extraction Temperature:

Temperatures ranging from 10 to 90 degrees Celsius were examined. To achieve a better balance between extraction kinetics and reduced solvent or analyte evaporation, an extraction temperature of 50 °C was determined to be ideal (42)(Figure 6E).

3.3 Optimization Conditions for MSPE Technique

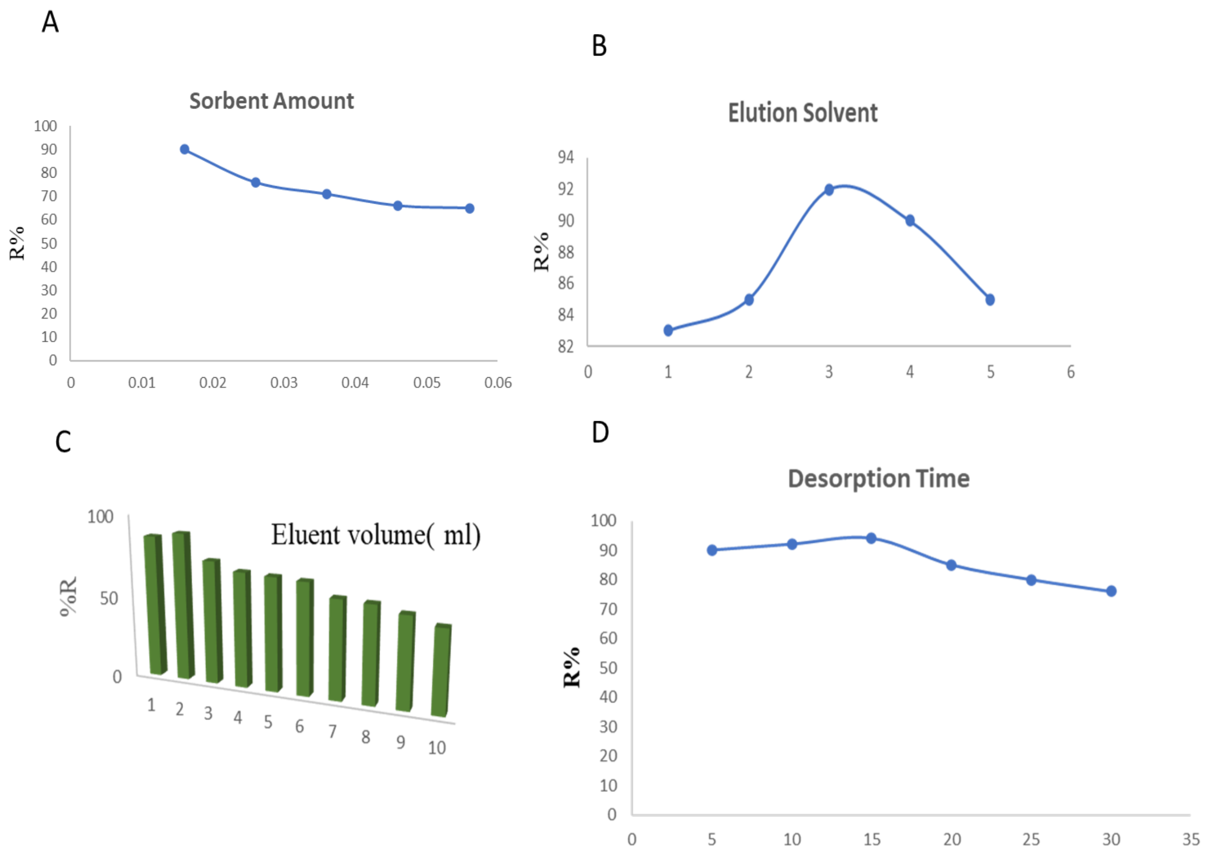

Figure 8: Sorbent Amount(A) Elution Solvent(B) Eluent Volume(C) Desorption Time(D)

After SHS-LLME, the magnetic solid-phase extraction (MSPE) process was improved to increase recovery and selectivity. Fe_3O_4 nanoparticles functionalized with oleic acid (Fe_3O_4@OA) served as the adsorbent. Adsorption and desorption processes were the main focus of optimization, and the following parameters were set:

3.3.1 Sorbent Amount:

Fe_3O_4@OA was tested at different concentrations ranging from 0.016 to 0.056 g. The highest extraction efficiency was achieved with a sorbent mass of 0.016 g; concentrations above this led to surface saturation and increased viscosity, preventing further gains as shown in Figure 8A.

3.3.2 Elution Solvent:

The ability of several solvents, including methanol, ethanol, acetonitrile, acetone, and toluene, to desorb DPH from Fe_3O_4@oleic acid nanoparticles was evaluated. Due to its high polarity, protic nature, and strong hydrogen bonding capabilities, methanol exhibited the greatest efficiency in breaking the interactions between the analyte and the sorbent surface. Consequently, methanol was selected as the optimal desorption solvent for the subsequent tests (see Figure 8B).

3.3.3 Eluent Volume

Eluent volumes ranging from 1 to 10 milliliters were examined. Full desorption of the analyte required only 2 mL of methanol, providing the best balance between volume efficiency and recovery (see figure 8C).

3.3.4 Desorption Time:

The study investigated the desorption efficiency over a time frame of 5 to 30 minutes. It was determined that 15 minutes is the optimal duration for ensuring complete release of the analyte into the elution solvent, based on the adsorption-desorption kinetics of magnetic sorbents, as illustrated in Figure 8D.

3.4 Method validation

Model solutions of DPH were prepared by spiking them with working standard solutions and analyzed using a combined SHS-LLME and MSPE procedure under optimized conditions. The calibration curve, represented by the equation \($y = 0.0021x - 0.0006$ \), exhibited excellent linearity over the concentration range of 2.5 to 25 mg/L, with a correlation coefficient (R^2) of 0.9996. The limit of detection (LOD) and limit of quantification (LOQ) were calculated using the formulas $LOD = 3.3 \times Sb / m$ and $LOQ = 10 \times Sb / m$, where (Sb) is the standard deviation of seven replicate measurements of the blank solution, and (m) is the slope of the calibration curve. Table 1 presents the LOD and LOQ values obtained from this analysis.

Due to the preconcentration factor of the method, the ratio of the initial sample volume to the final sample volume after extraction was significantly enhanced, demonstrating improved sensitivity and detection capabilities.

Table 1: The LOD and LOQ values for Diphenhydramine hydrochloride

Analyte	LOD	LOQ
DPH	1.30 mg/L	3.95 mg/L

4 Conclusion

To determine diphenhydramine hydrochloride (DPH), this study proposes an effective integrated microextraction method that combines magnetic solid-phase extraction (MSPE) with switchable hydrophilicity solvent-based liquid–liquid microextraction (SHS-LLME). The use of oleic acid-coated Fe_3O_4 nanoparticles enhances extraction efficiency due to their high surface area, stability, and magnetic properties. The robustness and reproducibility of the method were demonstrated by optimizing key parameters, leading to good selectivity and sensitivity with low solvent consumption. The method also exhibited high linearity and a low detection limit, confirming its analytical reliability. Furthermore, this approach aligns with green chemistry principles, making it a more environmentally friendly alternative to traditional extraction methods. These findings underscore the potential of the proposed method for routine DPH measurement in pharmaceutical formulations, paving the way for other applications in quality control and drug monitoring.

References

1. Holcomb IJ, Fusari SA. DIPHENHYDRAMINE HYDROCHLORIDE.
2. Khudair ZJ, Kadam ZM. Adsorption behavior of Chitosan-MWCNTS nanocomposite for the elimination of ofloxacin medication. Chem J Mold. 2024;19(1):84–92.
3. Hassan WS, El-Henawee MM, Gouda AA. Spectrophotometric determination of some histamine H1-antagonists drugs in their pharmaceutical preparations. Spectrochim Acta A Mol Biomol Spectrosc. 2008 Jan;69(1):245–55.
4. Tipparat P, Lapanantnoppakhun S, Jakmunee J, Grudpan K. Determination of diphenhydramine hydrochloride in some single tertiary alkylamine pharmaceutical preparations by flow injection spectrophotometry [Internet]. Vol. 30, Journal of Pharmaceutical and Biomedical Analysis. 2002. Available from: www.elsevier.com/locate/jpba
5. M. Kadam Z, M. Hadi H. Eco-friendly preparation of Moringa Oleifera Hydrogel nanocomposites as effective adsorbent for removal drug: Adsorption Isotherm. Journal of Nanostructures. 2023;(Articles in Press).
6. Yu C, Tang Y, Han X, Wu S. Flow injection chemiluminescence analysis of diphenhydramine hydrochloride and chlorpheniramine maleate. Instrum Sci Technol. 2006 Oct 1;34(5):529–36.
7. Marchesini AF, Williner MR, Mantovani VE, Robles JC, Goicoechea HC. Simultaneous determination of naphazoline, diphenhydramine and phenylephrine in nasal solutions by capillary electrophoresis [Internet]. Available from: www.elsevier.com/locate/jpba
8. Gomez MR, Sombra L, Olsina RA, Martínez LD, Silva MF. Development and validation of a capillary electrophoresis method for the determination of codeine, diphenhydramine, ephedrine and noscapine in pharmaceuticals. Farmaco. 2005 Jan;60(1):85–90.
9. Muller EE, Sherma J. Quantitative HPTLC determination of diphenhydramine hydrochloride in tablet, gelcap, and capsule antihistamine pharmaceuticals. J Liq Chromatogr Relat Technol. 1999;22(1):153–9.
10. Hasegawa C, Kumazawa T, Lee X, Fujishiro M, Kuriki A, Marumo A, et al. Simultaneous determination of ten antihistamine drugs in human plasma using pipette tip solid-phase extraction and gas chromatography/mass spectrometry. Rapid Communications in Mass Spectrometry: An International Journal Devoted to the Rapid Dissemination of Up-to-the-Minute Research in Mass Spectrometry. 2006;20(4):537–43.

11. Ye L, Stewart JT. HPLC determination of an ondan-setron and diphenhydramine mixture in 0.9% Sodium chloride injection. J Liq Chromatogr Relat Technol. 1996;19(5):711–8.
12. Tipparat P, Lapanantnoppakhun S, Jakmunee J, Grudpan K. Determination of diphenhydramine hydrochloride in some single tertiary alkylamine pharmaceutical preparations by flow injection spectrophotometry. J Pharm Biomed Anal. 2002;30(1):105–12.
13. M Hadi H, M Kadam Z. Economic Removal of Paracetamol drug from Aqueous Solution Using Olive Leaf Plant Hydrogel Nanocomposite as an Effective Adsorbent. Journal of Nanostructures. 2024;14(2):665–74.
14. Poole CF. New trends in solid-phase extraction. TrAC Trends in Analytical Chemistry. 2003;22(6):362–73.
15. Ullah N, Haseeb A, Tuzen M. Application of recently used green solvents in sample preparation techniques: A comprehensive review of existing trends, challenges, and future opportunities. Crit Rev Anal Chem. 2024;54(8):2714–33.
16. Whaib HA, Kadam ZM. Synthesis and characterization of a nano reagent and its use as a new type to inhibit alkaline phosphate enzyme, the study of the enzyme’s inhibitory kinetic properties and the study of its biological activity. In: AIP Conference Proceedings. AIP Publishing; 2023.
17. Seidi S, Rezazadeh M, Yamini Y. Pharmaceutical applications of liquid-phase microextraction. TrAC Trends in Analytical Chemistry. 2018;108:296–305.
18. Petcharoen K, Sirivat A. Synthesis and characterization of magnetite nanoparticles via the chemical co-precipitation method. Materials Science and Engineering: B. 2012 Mar 25;177(5):421–7.
19. Gupta R, Pancholi K, De Sa R, Murray D, Huo D, Droubi G, et al. Effect of Oleic Acid Coating of Iron Oxide Nanoparticles on Properties of Magnetic Polyamide-6 Nanocomposite. JOM [Internet]. 2019;71(9):3119–28. Available from: https://doi.org/10.1007/s11837-019-03622-5
20. Shahvandi SK, Banitaba MH, Ahmar H. Development of a new pH assisted homogeneous liquid-liquid microextraction by a solvent with switchable hydrophilicity: Application for GC-MS determination of methamphetamine. Talanta. 2018 Jul 1;184:103–8.
21. Taghvimi A, Hamishehkar H. Carbon coated magnetic nanoparticles as a novel magnetic solid phase extraction adsorbent for simultaneous extraction of methamphetamine and ephedrine from urine samples. J Chromatogr B Analyt Technol Biomed Life Sci. 2017 Jan 15;1041–1042:113–9.
22. Hassan RA, Tariq Z. Spectrophotometric determination of Amaranth dye using a two-step green cloud point and magnetic solid-phase extraction approach. Engineering Proceedings. 2024;59(1):244.

23. Whaib HA, Kadam ZM. Synthesis and characterization of a nano reagent and its use as a new type to inhibit alkaline phosphate enzyme, the study of the enzyme's inhibitory kinetic properties and the study of its biological activity. In: AIP Conference Proceedings. AIP Publishing; 2023.
24. Mahdavi M, Ahmad M Bin, Haron MJ, Namvar F, Nadi B, Ab Rahman MZ, et al. Synthesis, surface modification and characterisation of biocompatible magnetic iron oxide nanoparticles for biomedical applications. Molecules. 2013 Jul;18(7):7533–48.
25. Alradaa ZAA, Kadam ZM. X-ray diffraction Characterization of crystalline structure regent4 (4-Sulphophenyl Azo) Pyrogallol. In: Journal of Physics: Conference Series. IOP Publishing; 2021. p. 012012.
26. Gupta R, Pancholi K, De Sa R, Murray D, Huo D, Droubi G, et al. Effect of Oleic Acid Coating of Iron Oxide Nanoparticles on Properties of Magnetic Polyamide-6 Nanocomposite. JOM. 2019 Sep 15;71(9):3119–28.
27. Senturk F, Cakmak S, Ozturk G. Synthesis and Characterization of Oleic Acid Coated Magnetic Nanoparticles for Hyperthermia Applications. Natural and Applied Sciences Journal. 2019 Dec 31;2:16–29.
28. Mahdavi M, Ahmad M Bin, Haron MJ, Namvar F, Nadi B, Ab Rahman MZ, et al. Synthesis, surface modification and characterisation of biocompatible magnetic iron oxide nanoparticles for biomedical applications. Molecules. 2013 Jul;18(7):7533–48.
29. Laurent S, Forge D, Port M, Roch A, Robic C, Vander Elst L, et al. Magnetic iron oxide nanoparticles: synthesis, stabilization, vectorization, physicochemical characterizations, and biological applications. Chem Rev. 2008;108(6):2064–110.
30. Kadam ZM, Flieh SS. AFM and Fe-SEM imaging applications of functionalized carbon nanotubes in drug delivery systems of folic acid. In: AIP Conference Proceedings. AIP Publishing; 2024.
31. Synthesis of Magnetic Nanoparticles of Fe_sub_3__sub_O_sub_4__sub_ and CoFe_sub_2__sub_O_sub_4__sub_ and Their Surface Modification by Surfactant Adsorption.
32. Sun S, Zeng H. Size-controlled synthesis of magnetite nanoparticles. J Am Chem Soc. 2002 Jul 17;124(28):8204–5.
33. Yang K, Peng H, Wen Y, Li N. Re-examination of characteristic FTIR spectrum of secondary layer in bilayer oleic acid-coated Fe 3 O 4 nanoparticles. Appl Surf Sci. 2010 Mar 1;256(10):3093–7.
34. Mahdavi M, Ahmad M Bin, Haron MJ, Namvar F, Nadi B, Ab Rahman MZ, et al. Synthesis, surface modification and characterisation of biocompatible magnetic iron oxide nanoparticles for biomedical applications. Molecules. 2013 Jul;18(7):7533–48.

35. Sun C, Lee JSH, Zhang M. Magnetic nanoparticles in MR imaging and drug delivery. Vol. 60, Advanced Drug Delivery Reviews. 2008. p. 1252–65.
36. Wei Y, Han B, Hu X, Lin Y, Wang X, Deng X. Synthesis of Fe3O4 nanoparticles and their magnetic properties. In: Procedia Engineering. Elsevier Ltd; 2012. p. 632–7.
37. Do BPH, Nguyen BD, Nguyen HD, Nguyen PT. Synthesis of magnetic composite nanoparticles enveloped in copolymers specified for scale inhibition application. Advances in Natural Sciences: Nanoscience and Nanotechnology. 2013;4(4).
38. Muntaka M, Anwarul Kabir Bhuiya M, Nasrin J, Madbar S, Niva M, Uddin B, et al. Enhancing Biomedical Potential: Comparative Analysis of Oleic Acid-Coated and Uncoated Iron Oxide Nanoparticles through Synthesis and Characterization [Internet]. Available from: https://ssrn.com/abstract=4572858
39. Malaeru T, Patroi E, Virgil M, Oprea O, Patroi D, Morari C, et al. Preparation and Characterization of Fe3O4 Magnetic Nanofluid in Vegetable Oil. Revista de Chimie. 2019 Mar 15;70:459–64.
40. Jessop PG, Heldebrant DJ, Li X, Eckert CA, Liotta CL. Reversible nonpolar-to-polar solvent. Nature. 2005;436(7054):1102.
41. Shahvandi SK, Banitaba MH, Ahmar H. Development of a new pH assisted homogeneous liquid-liquid microextraction by a solvent with switchable hydrophilicity: Application for GC-MS determination of methamphetamine. Talanta. 2018;184:103–8.
42. Jessop PG, Phan L, Carrier A, Robinson S, Dürr CJ, Harjani JR. A solvent having switchable hydrophilicity. Green Chemistry. 2010;12(5):809–14.
43. Javadian S, Sadrpoor SM. Functionalized graphene oxide with core-shell of Fe3O4@ oliec acid nanospheres as a recyclable demulsifier for effective removal of emulsified oil from oily wastewater. Journal of Water Process Engineering. 2019;32:100961.